Journal of Marine Science and Technology, Vol. 25 No. 1 pp. 54-61 (2017)
DOI: 10.6119/JMST-016-0811-1

A PARAMETRIC STUDY OF AN IMPLEMENTING ADAPTIVE TIME REVERSAL MIRROR AS A CROSSTALK MECHANISM FOR UNDERWATER COMMUNICATION

Yi-Wei Lin and Gee-Pinn Too

Key words: time reversal mirror, adaptive time reversal mirror, finite impulse response filter, underwater communication.

ABSTRACT

The time reversal mirror technique has been widely applied to mitigate the inter-symbol interference in underwater channels. Meanwhile, an adaptive time reversal mirror is introduced to improve the crosstalk quality between receivers in underwater acoustic communication (UAC). However, array configuration affects the performance of this mechanism. To explore the effectiveness of this method, this study extended the analysis of adaptive time reversal mirror as a crosstalk mechanism and explored the mechanism in an experiment using a towing tank as a testing platform. The advantage of this process is its simplicity in examining the effects of the array configuration of this crosstalk mechanism. Results of parametric experiments are discussed i.e., the effects of signal to noise ratio in a single and multi-channel, number of receivers, spacing between sources and noise energy threshold. Experimental data at 10 and 16 kHz with a 5-kHz bandwidth demonstrate as much as an 8-dB signal to noise ratio improvement for four receivers dual sources over a 30 m communication range in a 3.3 m depth testing platform. The results indicate that adaptive time reversal mirror has better performance when the number of receivers increases. Overall, the performance of adaptive time reversal mirror is better than time reversal mirror in terms of BER and SNR. Also, the array configuration such as number of receivers and spacing between sources affects the performance of SNR and BER. This technique can be applied as the alternative way to increase the data rate at short ranges for multiple-input-multiple-output communication applications.

Paper submitted 08/20/15; revised 04/04/16; accepted 08/11/16. Author for correspondence: Yi-Wei Lin (e-mail: ls5028@gmail.com).
Department of Systems and Naval Mechatronic Engineering, National Cheng Kung University, Tainan, Taiwan, R.O.C.

I. INTRODUCTION

Recently, underwater acoustic communication has been widely developed by researchers and professionals in many aspects, such as for channel modeling, signal processing techniques, environmental conditions and suitable equalizer applications. The most challenging effect in underwater communication is the multipath effect from the interaction between acoustic signals and boundary conditions. This multipath effect induces severe inter-symbol interference (ISI) in the communication process and reduces the quality of the communication. The time reversal mirror (TRM) approach has been applied to solve this problem and mitigate ISI in underwater acoustic environments (Kuperman et al., 1998; Song et al., 1998; Dungan et al., 2000; Edelmann et al., 2002; Edelmann et al., 2005). Time reversal was originally used as an alternative equalization for channel distortion (Fink et al., 1989) and the development of time reversal for selective focusing on two scatters using a decomposition operator was explored by Prada et al. (1996).

The application of time reversal in multiple-input multiple-output systems to increase the data rate was discussed (Song et al., 2006). TRM was further developed (Kim et al., 2001). They used an adaptive weighting on the TRM array and demonstrated a selective focusing in free space, and named it adaptive time reversal mirror (ATRM). Kim and Shin (2003) improved and applied ATRM for nulling crosstalk between receivers by sending out independent symbol sequences simultaneously to different receivers. Via the adaptivity concept, Song et al. (2005 and 2006) explored the weighting vector on the TRM in order to minimize the acoustic energy incident on the corresponding scattering interface due to rough water-bottom interface. Furthermore, Song et al. (2010) applied ATRM for additional suppression of crosstalk among users in multiuser underwater communication. Their results showed that ATRM increased the signal to noise ratio (SNR) from three-user communication in long-range communication.

In the present study, we extend the analysis of ATRM and consider the effect of array configuration, transmission frequency and some parametric studies. Then, we describe how these ef-

fects affect the performance of TRM and ATRM in underwater acoustic communication. ATRM was explored in an 8 m × 4 m × 175 m towing tank as an underwater communication testing platform. Due to the boundary condition, the towing tank has a strong multipath effect that makes it very challenging and thus constitutes a suitable testing platform to investigate underwater acoustic communication. However, an advantage is that the tank enables easy setup of the array configuration in relation to the testing platform depth. Parametric studies are discussed by comparing and analyzing the results from the experiments in the tank i.e., the effect of SNR with respect to single and multi-channels, number of receivers, spacing between sources and noise energy threshold. In the experiments, two different carrier frequencies (fc) 10 kHz and 16 kHz were transmitted from two sources to the four receivers with adjustable array configuration to explore the multiple communication and cross-talking approach by using TRM and ATRM. The remainder of this paper is organized as follows: Section II describes the methodology of TRM, ATRM and the adaptive digital filter. Section III presents the experimental results, while Section IV compares those results to evaluate the effectiveness of ATRM. Finally, Section V offers conclusions and recommendations for future research.

II. METHODOLOGY

1. Time-Reversal Mirror

Consider a two-source and m^{th} receivers system, in which $s_1(t)$ and $s_2(t)$ are the target source signal and the noise source signal, respectively. The received signal by the m^{th} receiver is $p_m(t)$. The environment impulse response functions between the target sources, the noise source and the m^{th} receiver are $g_m^1(t)$ and $g_m^2(t)$. Furthermore, the output of TRM $O_{TRM}(t)$ can be expressed as the following equation:

$$\begin{aligned} O_{TRM}(t) &= \sum_{m=1}^{M} g_m^1(-t) \otimes p_m(t) \\ &= \sum_{m=1}^{M} g_m^1(-t) \otimes g_m^1(t) \otimes s_1(t) \\ &\quad + \sum_{m=1}^{M} g_m^1(-t) \otimes g_m^2(t) \otimes s_2(t) \end{aligned} \tag{1}$$

where ⊗ denotes convolution integration. Via the self-focusing property, the target signal can be restored by TRM ($\sum_{m=1}^{M} g_m^1(-t) \otimes g_m^1(t) \otimes s_1(t)$), which corresponds to the first term of the right-hand side (RHS) of Eq. (1), as described in Prada et al. (1996). The interference of noise signals can be reduced by the summation effect of the receiver array ($\sum_{m=1}^{M} g_m^1(-t) \otimes g_m^2(t) \otimes s_2(t)$), which corresponds to the second term of the RHS of (1). The performance of the noise reduction is governed by the number of receivers (m); however, the interference of noise signals can not be perfectly canceled because the number of receivers is limited.

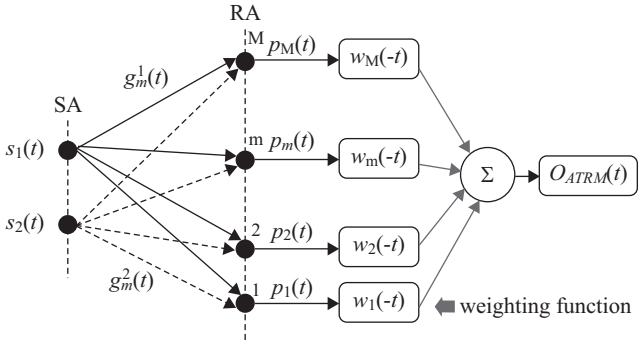

Fig. 1. Schematic diagram of adaptive time reversal mirror.

2. Adaptive Time-Reversal Mirror

In the adaptive time reversal mirror (ATRM) approach, the impulse response function of time-reversal $g^1(-t)$ is replaced with an adaptive weighting function of time-reversal $w(-t)$. The time-domain output $O_{ATRM}(t)$ and the frequency-domain $O_{ATRM}(\omega)$ can be expressed by the equations below, and the schematic diagram can be represented as in Fig. 1.

$$\begin{aligned} O_{ATRM}(t) &= \sum_{m=1}^{M} w_m(-t) \otimes p_m(t) \\ &= \sum_{m=1}^{M} w_m(-t) \otimes g_m^1(t) \otimes s_1(t) \\ &\quad + \sum_{m=1}^{M} w_m(-t) \otimes g_m^2(t) \otimes s_2(t) \end{aligned} \tag{2}$$

$$O_{ATRM}(\omega) = \mathbf{W}^H \mathbf{G_1} \mathbf{S_1} + \mathbf{W}^H \mathbf{G_2} \mathbf{S_2} \tag{3}$$

where $\mathbf{W}$ is an adaptive weighting vector (M × 1), while $\mathbf{G}_1$ and $\mathbf{G}_2$ are frequency response vectors of the environment (M × 1) between the target source, the noise source and the receivers, respectively. $\mathbf{S}_1$ and $\mathbf{S}_2$ are the target source signal and the noise source signal in frequency-domain, respectively, and H denotes the Hermitian transpose of a vector. Suppose that can restore the target source signal $\mathbf{S}_1$ and reduce the noise source signal $\mathbf{S}_2$, according to a reference (Kim et al., 2004), the objective function and the constraint condition are also defined as the following equation in this optimization problem:

$$\min_{W} \mathbf{W}^H \mathbf{K} \mathbf{W} \quad subject \quad to \quad \mathbf{W}^H \mathbf{C} = \mathbf{F} \tag{4}$$

where $\mathbf{K}$ is a cross-spectral density matrix (CSDM), $\mathbf{C} = [\mathbf{G}_1, \mathbf{G}_2]$ is a constraint matrix (M × 2), and $\mathbf{F} = \{10\}$ is a response vector (1 × 2). According to the definition from linearly constrained minimum variance (LCMV), the optimization solution of $\mathbf{W}$ is derived as follows:

Table 1. Experimental conditions and parameter settings.

Conditions and Parameters	Symbols	Values
Water Depth	D_W	3.3 m
Width	W_W	8 m
Length	L_W	170 m
Communication Range	R	30 m
Spacing between Receivers	d_{RA}	20 cm
Number of Sources	n	2
Carrier Frequencies	f_C	10 kHz &16 kHz
Number of Receivers	m	1-4
Noise energy threshold	TH	0%, 10%, 30%, 50%
Spacing between Sources	d_{SA}	4 cm, 6 cm, 12 cm, 17 cm

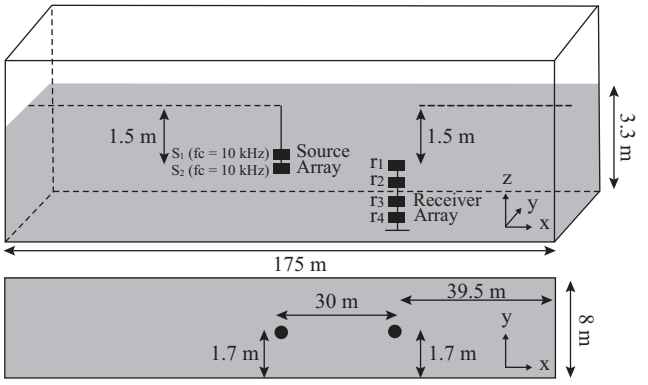

Fig. 2. The array configuration in underwater communication testing platform.

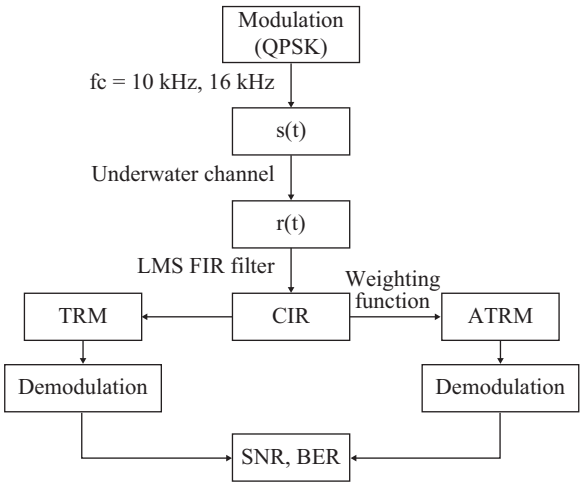

Fig. 3. The underwater communication process with TRM or ATRM.

$$\mathbf{W} = \mathbf{K}^{-1}\mathbf{C}\left(\mathbf{C}^{H}\mathbf{K}^{-1}\mathbf{C}\right)^{-1}\mathbf{F} \tag{5}$$

when impulse response functions of the environment between the target source, the noise sources, and the receiver array are known, the frequency response functions of environment are calculated via fast fourier transform (FFT) first. Next, the optimal adaptive weighting vector (**W**) is calculated by using (5); finally, the optimal adaptive weighting function $w(t)$ is calculated via inverse fast fourier transform (IFFT). When the signals are received from the target source and the noise source by the receiver array, the target signal $s_1(t)$ is restored and the noise signal $s_2(t)$ is canceled through (2).

III. EXPERIMENT

1. Experimental Process

To verify the proposed process, an underwater channel was realized in a testing platform measuring 175 m in length, 8 m in width and 3.3 m in depth, as shown in Fig. 2. A multiple-input and multiple-output (MIMO) array configuration is explored by using 6 transducers, 2 of which are used as 2 sources and the rest as receivers. It was deployed at an approximate depth of 1.2 m, with the maximum water depth in the channel being around 3.3 m. A picture of the experimental setup is depicted in Fig. 2.

As described in the introduction, parametric studies are analyzed in this research i.e., the effects of the number of receivers (m), spacing between sources (d_{SA}) and noise energy threshold (TH), as shown in Table 1. Quadrature phase-shift keying (QPSK) signals were modulated from sources to receivers with a carrier frequency of 10 kHz at 101 dB re 1 μPa for source no. 1 and 16 kHz at 103 dB re 1 μPa for source no. 2. channel impulse response (CIR) was calculated via a FIR least mean squares (LMS) filter, which has the advantages of providing stability and a linear phase response. TRM and ATRM are proposed to focus energy, and thus mitigate the effects of the multipath dispersion and minimize ISI. These parameters are analyzed by considering the SNR to understand the effect of the noise reduced by the equalizer. The values of SNR and bit error rate (BER) are the indexes to evaluate the communication quality. The underwater communication process at the testing platform based on the description above is shown in Fig. 3.

Table 1 shows the experiment conditions and parameters. In the experiment, a 30 m range of communication was performed

Table 2. The comparison of SNR of CIR, after TRM and after ATRM processing.

Channel number	SNR of CIR		SNR (After TRM processing)		SNR (After ATRM processing)	
	Source no. 1	Source no. 2	Source no. 1	Source no. 2	Source no. 1	Source no. 2
1	15	11.7	1.5	2.8	1.6	2.8
2	18.2	14.4	5.3	5.8	2.6	4.6
3	16.9	13.6	1.9	5.7	1.9	5.9
4	10	7	-2.8	-4.1	0.8	3

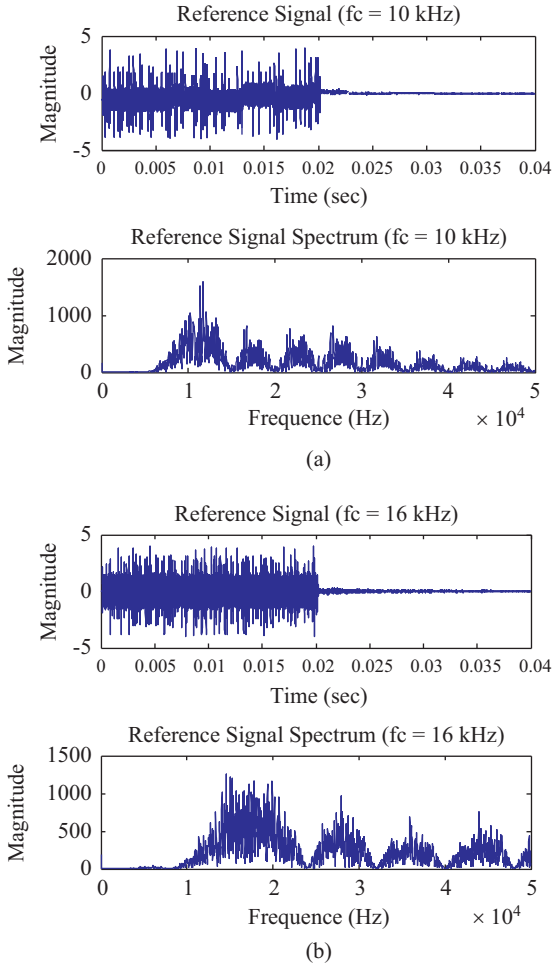

Fig. 4. The time series and magnitude spectrum of the reference signal for (a) 10 kHz and (b) 16 kHz.

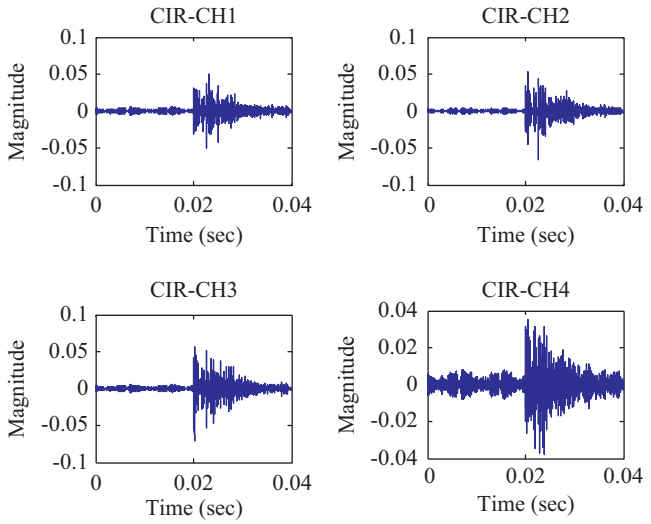

Fig. 5. Channels impulse response between four receivers to source no. 2 (16 kHz).

with a spacing between sources (d_{SA}) of 17 cm and spacing between receivers (d_{RA}) of 20 cm. The QPSK signals shown in Fig. 4 are 2 ms in duration with 200 and 320 bits binary data for the two source signals, respectively. The testing platform provides the multi-path effect in the received signal. The testing platform surface condition is assumed as a pressure-release boundary. Fig. 4 shows the reference signals from source no. 1(a) and source no. 2(b). Since these bandwidths are similar, they cannot be separated by a frequency domain filter.

Furthermore, the channel impulse response (CIR) from each receiver is given in Fig. 5. Fig. 5 indicates that the testing platform has a strong multipath effect due to the interaction between the signal and boundary of the testing platform. The CIR is trained by using chirp signal and processed using an FIR filter. Note that Fig. 5 only show the CIR from the 16 kHz source signal. The signal and constellation diagram comparison between the ATRM and TRM processes for the 10 kHz source signal are respectively shown in Figs. 6 and 7 which indicate that the SNR and bits error rate (BER) performance of ATRM are superior to those of the TRM process. The SNR of ATRM is around 9.7 dB and BER is 0, while the SNR of TRM is around 2.4 dB and BER is 0.12.

IV. PARAMETRIC ANALYSIS

1. Effect of SNR for Single Channel Case

In this study, the SNR and BER of the single channel at each receiver array were analyzed. The first analysis was observed SNR of CIR at each channel in order to check the performance of channel condition. Table 2 shows the comparison of signal of noise ratio of CIR, after time reversal and adaptive time reversal processes. The chirp signal was used as the training signal with the spacing between two sources (d_{RA}) set at 17 cm and the carrier frequency are 10 kHz and 16 kHz for source no. 1 and no. 2, respectively. Table 2 indicates that receiver no. 4 has

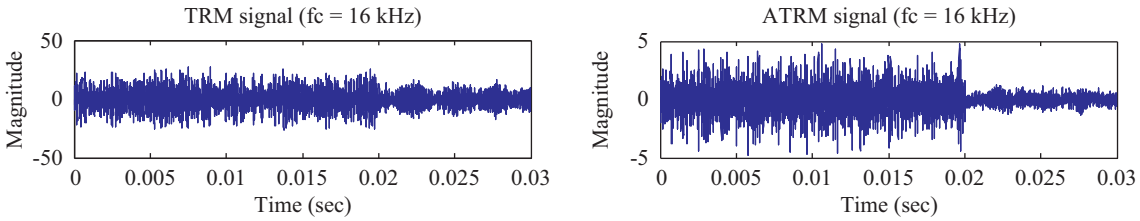

Fig. 6. TRM & ATRM signal for 16 kHz using four receivers.

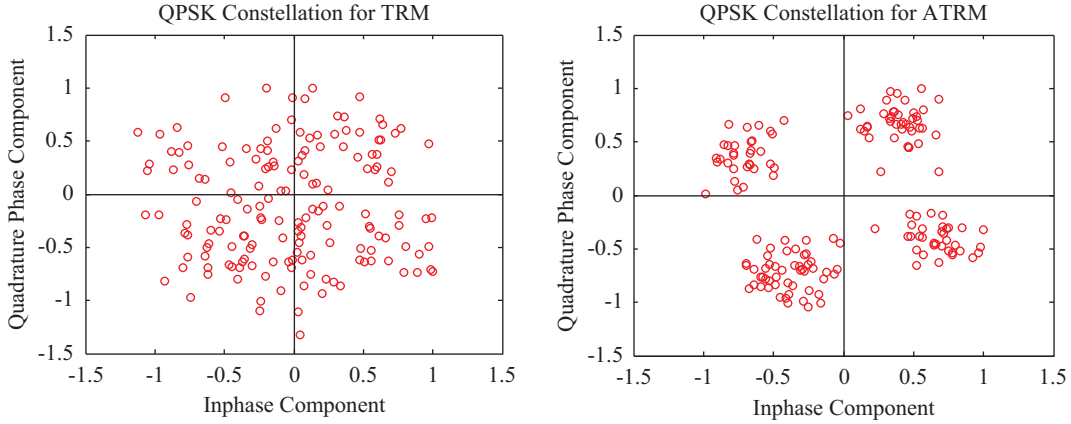

Fig. 7. TRM & ATRM QPSK constellation diagram.

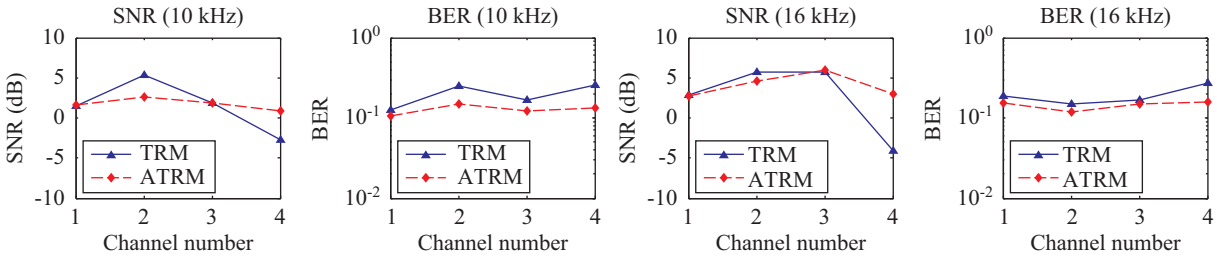

Fig. 8. The SNR and BER performance of single channel.

the lowest performance, for which the SNR is less than 10 dB. Fig. 8 shows the comparison of SNR and BER between the TRM and ATRM processes. In the SNR comparison, the performance of the ATRM is similar to TRM. Furthermore, the overall BER performance of ATRM is better than that of TRM. However, BERs are similar at channels 2 and 4, but SNR is 8 dB different for source 1. It shows that the noise affects the TRM process notability and the communication quality improvement is limited in single channel case. Also, it can be concluded that ATRM has the advantage of removing noise from the other source channel, even if channel no. 4 has low performance. The unique behavior in channel no. 4, in which the SNR performance after the TRM process was always less than zero due to the SNR of CIR is less than 10 dB. Meanwhile, the BER performance is always higher than the other channels after the ATRM process, as shown in Fig. 8. Therefore, the performance of channel no. 4 has been greatly improved after the ATRM process and SNR of CIR was an important factor for TRM and ATRM performances.

2. Effect of Number of Receivers (m) for Multi-Channel Case

The SNR and BER performance between ATRM and TRM in multi-channel consideration are analyzed in this case. This case used the same carrier frequencies of sources, range of communication, d_{SA} and d_{RA} as in the previous case. The performance comparison is shown in Fig. 9. In the SNR performance analysis, the results show that ATRM has better performance than TRM. When the number of receiver increases, SNR increases; meanwhile, the BER is reduced when the number of receivers increases. This is because the low performance of channel no. 4 affects the overall time reversal process. In BER performance analysis, the adaptive time reversal process always has better performance than time reversal process. Both adaptive and time reversal processes have the characteristic of when

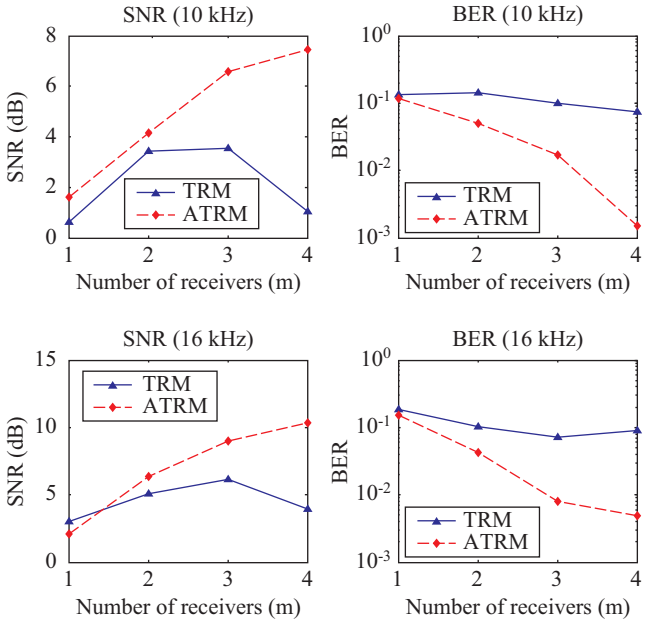

Fig. 9. SNR and BER performances versus number of receivers for TRM and ATRM.

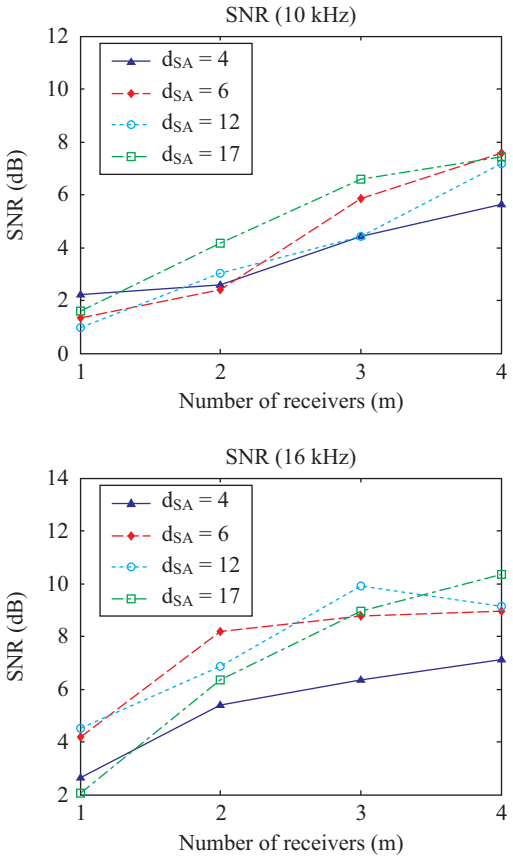

Fig. 10. SNR performance with number of receivers at variation of spacing between sources (d_{SA}).

number of receivers increases, the BER reduces with ATRM to

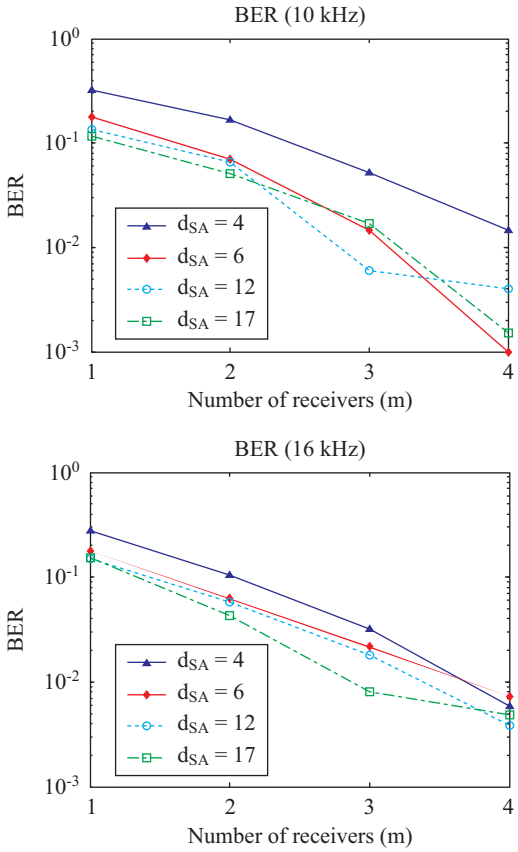

Fig. 11. BER performance with number of receivers at variation of spacing between sources (d_{SA}).

around 0.15-0 and TRM around 0.2-0.05.

From the results of Fig. 9, it can be concluded that the adaptive time reversal process offers the characteristic of noise-reduction and has a better performance when the array number increases for a two-source setup. But, one of the valuable features of TRM is its robustness, i.e., graceful degradation in the presence of mismatches and perturbations.

3. Effect of Spacing Between Sources (d_{SA})

Some variations of spacing between sources (d_{SA}) are analyzed in this case, namely at 4 cm, 6 cm, 12 cm and 17 cm. In the present study, two carrier frequencies 10 kHz and 16 kHz were used and the wavelengths correspond to 15 cm and 9.37 cm, respectively. Therefore, spacing between sources for this case were set to be below 1/2 the wavelength ($\lambda/2$) as well as above one wavelength (λ). The purpose was to determine the best performance of array distance configuration in the ATRM process. By using the same procedure as the previous cases, the performance comparison of SNR and BER are shown in Figs. 10 and 11. As can be seen, when the distance between sources (d_{SA}) increases, the SNR increases to 3.5-8 dB and BER reduces. Meanwhile, the performance also increases when the number of receivers (m) increases. Good communication performance can be achieved when the SNR is around

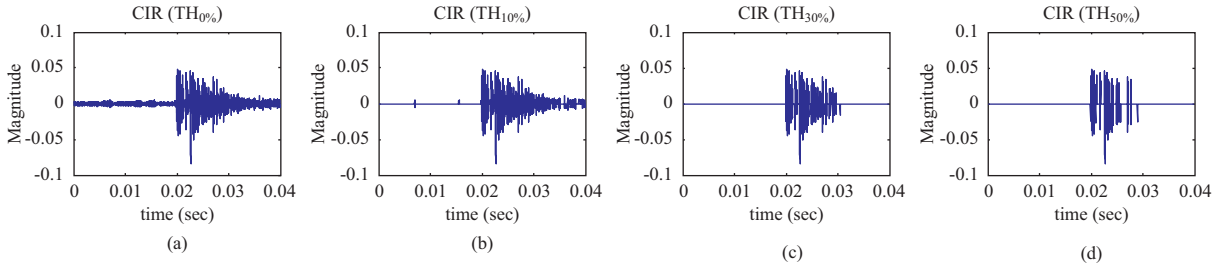

Fig. 12. The CIR of energy reduction of E_d for channel no. 1 to source no. 1 (fc = 10 kHz).

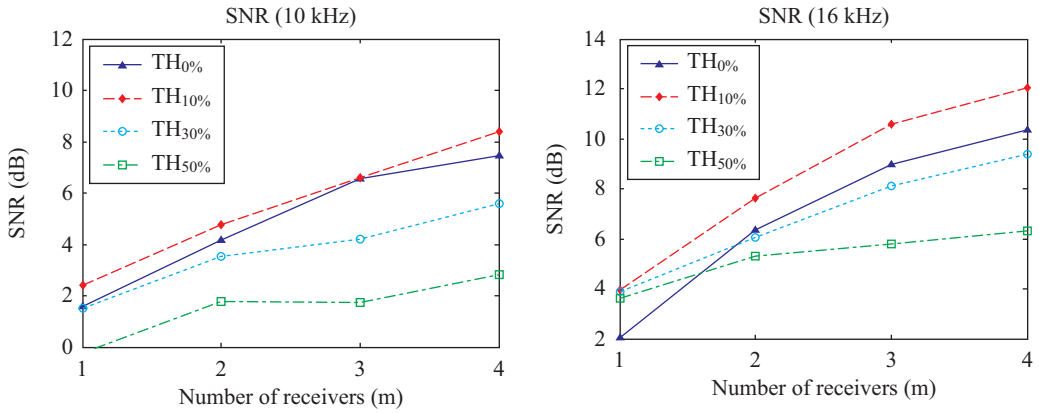

Fig. 13. The SNR performance of noise energy threshold (TH) for ATRM The underwater communication process with TRM or ATRM.

8 dB. When spacing between sources (d_{SA}) is smaller than λ/2, the result is still applicable. This observation can be applied as the alternative way to increase the data rate in short ranges for multiple-input and multiple-output (MIMO) communication applications.

4. Effect of Noise Energy Threshold (TH)

In order to reduce the noise effect in the CIR and improve the calculation speed in the calculation process, we define a noise energy threshold percentage of direct path energy (TH) as

$$\text{TH } \% = \frac{\textit{Noise energy}}{\textit{direct path energy } (E_d)} \times 100\% \qquad (6)$$

The effect of noise energy threshold percentages of direct path energy (E_d) is analyzed by simplifying CIR in this case. Four different noise energy thresholds for E_d reducing percentages are considered in the calculation process. These reduction percentages are shown in Figs. 12(a)-(d), where Fig. 12(a) is the normal CIR without energy reduction and is denoted as $Th_{0\%}$. Accordingly, $Th_{10\%}$, $Th_{30\%}$, $Th_{50\%}$ represents 10%, 30% and 50% reductions of E_d, as shown in Figs. 12(b-d) respectively. Fig. 13 shows the CIR by using chirp signals in the adaptive time reversal process for CH1 to source no. 1. The CIR itself is the results from 30 m ranges of communication with the spacing of sources (d_{SA}) being 17 cm and spacing of receivers (d_{RA}) 20 cm. Two different carrier frequencies are transmitted in the channels i.e., 10 kHz and 16 kHz for source 1 and 2, respectively. After the reduction percentages of direct path energy of CIR are determined, the comparison of BER and SNR for ATRM with consideration to these reduction percentages is shown in Figs. 13 and 14.

As shown in Figs. 13 and 14, it can be concluded that the 10% noise energy threshold has better SNR and BER performance than without using a noise energy threshold ($TH_{0\%}$). Because, during the signal transmission, CIR accuracy is affected by measurement errors from receiver's thermal noise and ambient noise. 10% noise reduction threshold provides a better CIR accuracy, and has better SNR and BER performance.

Furthermore, the 30% and 50% noise energy threshold reduce the CIR accuracy, and BER become 0.016 and 0.055 when number of receivers (m) is 4. These results suggest that if the SNR after ATRM rises above 6 dB, BER is then close to 0.

V. CONCLUSION

In this study, we tested the implementation of ATRM as a crosstalk mechanism for underwater communication in a towing tank as an underwater channel. Various cases were discussed by the experimental analysis with respect to the effects of SNR in the single and multi-channel, number of receivers, spacing between sources and noise energy threshold. Based on the experimental results, it can be concluded that ATRM has the characteristic of noise-reduction and has a better performance when the number of receivers increases. Overall, the performance of adaptive time reversal mirror is better than time reversal mirror in terms of BER and SNR. The other advantage of experi-

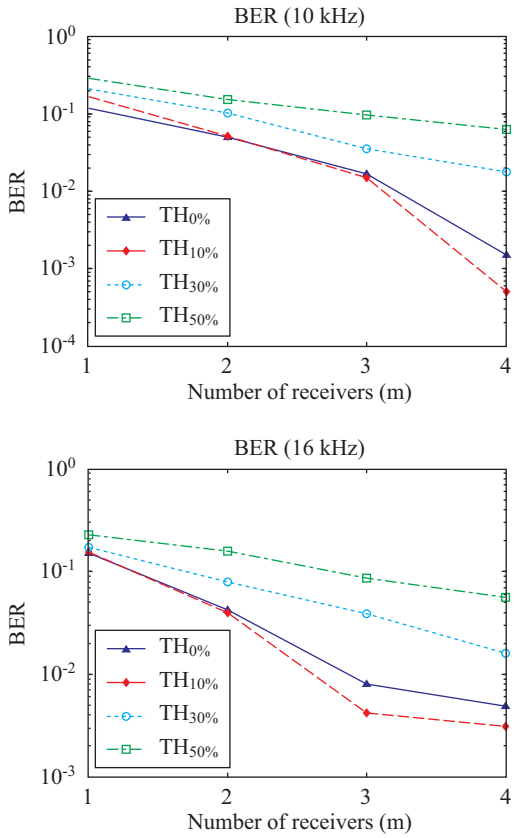

Fig. 14. The BER performance of noise energy threshold (TH) for ATRM The underwater communication process with TRM or ATRM.

mental process by using a towing tank as a testing platform is that it is easier to examine the effects of the array configuration of the crosstalk mechanism. The noise energy threshold for direct path energy in CIR is important in order to minimize the noise effect. An interesting result of this study is that this technique can be applied as an alternative way to increase the data rate in short ranges of MIMO communication applications by setting up the spacing between sources (d_{SA}) to be smaller than $\lambda/2$ wavelength. However, better estimation of CIR is needed in order to improve the communication quality using this method and the crosstalk mechanism. In the future, a combination between ATRM and adaptive equalization can be considered as an improvement of this study in order to provide better estimation of CIR and improvements to the communication quality.

REFERENCES

Dungan, M. R. and D. R. Dowling (2000). Computed narrow-band time reversing array retrofocusing in a dynamic shallow ocean. Journal of Acoustical Society of America 107, 3101-3112.

Edelmann, G. F., H. C. Song, S. Kim, W. S. Hodgkiss, W. A. Kuperman and T. Akal (2005). Underwater acoustic communication using time reversal. IEEE Journal of Oceanic Engineering 30, 852-864.

Edelmann, G. F., T. Akal, W. S. Hodgkiss, S. Kim, W. A. Kuperman and H. C. Song (2002). An initial demonstration of underwater acoustic communication using time reversal mirror. IEEE Journal of Oceanic Engineering 27, 602-609.

Fink, M., C. Prada, F. Wu and D. Cassereau (1989). Self focusing in inhomogeneous media with time reversal acoustic mirrors. Proceeding of IEEE Ultrasonic symposium 2, 681-686.

Kim, J. S. and K. C. Shin (2004). Multiple focusing with adaptive time-reversal mirror. Journal of Acoustical Society of America 115, 600-606.

Kim, J. S. and K. C. Shin (2003). Nulling crosstalk in underwater communication with an adaptive time reversal mirror. Proceeding of IEEE Oceans Conference 3, 1382-1388.

Kim, J. S., H. C. Song and W. A. Kuperman (2001). Adaptive time reversal mirror. Journal of Acoustical Society of America 109, 1817-1825.

Kuo, S. M. and D. R. Morgan (1996). Active Noise Control Systems: Algorithms and DSP Implementations. John Wiley & Sons, New York.

Kuperman, W. A., W. S. Hodgkiss, H. C. Song, T. Akal, C. Ferla and D. R. Jackson (1998). Phase conjugation in the ocean: Experimental demonstration of an acoustic time reversal mirror. Journal of Acoustical Society of America 103, 25-33.

Prada, C., S. Manneville, D. Spoliansky and M. Fink (1996). Decomposition of the time reversal operator: Detection and selective focusing on two scatters. Journal of Acoustical Society of America 99, 2067-2076.

Song, H. C., J. S. Kim, W. S. Hodgkiss, W. A. Kuperman and M. Stevenson (2010). High rate multiuser communication in shallow water. Journal of Acoustical Society of America 128, 2920-2925.

Song, H. C., P. Roux, W. S. Hodgkiss, W. A. Kuperman, T. Akal and M. Stevenson (2006). Multiple-input-multiple output coherent time reversal communications in a shallow water acoustic channel. IEEE Journal of Oceanic Engineering 31, 170-178.

Song, H. C., W. A. Kuperman and W. S. Hodgkiss (1998). A time reversal mirror with variable range focusing. Journal of Acoustical Society of America 103, 3234-3240.

Song, H. C., W. S. Hodgkiss, W. A. Kuperman, M. Stevenson and T. Akal (2006). Improvement of time reversal communications using adaptive channels equalizers. IEEE Journal of Oceanic Engineering 31, 487-496.

Song, H. C., W. S. Hodgkiss, W. A. Kuperman, P. Roux, T. Akal and M. Stevenson (2005). Experimental demonstration of adaptive reverberation nulling using time reversal mirror. Journal of Acoustical Society of America 118, 1381-1387.